Journal of Inflammation Research

Dovepress
open access to scientific and medical research

Open Access Full Text Article

ORIGINAL RESEARCH

Protective Effect of Qingchang Wenzhong Decoction on Colitis and Colitis-Related Carcinogenesis by Regulating Inflammation and Intestinal Fibrosis

Yuan Cheng[1,2], Junxiang Li[1], Xiaosi Zhang[1], Yalan Li[3], Xiaojun Shi[1], Rui Shi[1], Tangyou Mao[1], Fushun Kou[1,4], Lei Shi[1]

[1]Gastroenterology Department, Dongfang Hospital, Beijing University of Chinese Medicine, Beijing, 100078, People's Republic of China; [2]School of Traditional Chinese Medicine & School of Integrated Chinese and Western Medicine, Nanjing University of Chinese Medicine, Nanjing, 210046, People's Republic of China; [3]School of Life Sciences, Beijing University of Chinese Medicine, Beijing, 100029, People's Republic of China; [4]Center for IBD Research, Department of Gastroenterology, Shanghai Tenth People's Hospital, School of Medicine, Tongji University, Shanghai, 200072, People's Republic of China

Correspondence: Lei Shi, Department of Gastroenterology, Dongfang Hospital, Beijing University of Chinese Medicine, No. 6, 1st Section, Fangxingyuan, Fangzhuang, Fengtai District, Beijing, 100078, People's Republic of China, Email b01350@bucm.edu.cn; Fushun Kou, Center for IBD Research, Department of Gastroenterology, The Shanghai Tenth People's Hospital, Tongji University, No. 301 Yanchang Road, Shanghai, 200072, People's Republic of China, Email koufuhsun@126.com

Purpose: Ulcerative colitis (UC) is a chronic inflammatory bowel disease characterized by mucosal inflammation, which may develop into ulcerative colitis-associated carcinogenesis (UCAC) with disease progression. Qingchang Wenzhong Decoction (QCWZD) is a classic and effective prescription for the clinical treatment of UC. QCWZD has been shown to alleviate intestinal mucosal injury in acute and chronic UC models. This study aimed to explore and then verify the pharmacological mechanisms of QCWZD in UC and UCAC therapy.

Methods: In this study, approaches including microarray analysis, network pharmacology, and biological verification are employed to clarify the mechanism of QCWZD in the treatment of UC and UCAC. TCMSP, Swiss Target Prediction, and Similarity Ensemble Approach were used to investigate the active ingredients and targets of QCWZD. UC and UCAC valid targets were identified by the microarray data in the GEO database (GSE38713 and GSE47908). The core targets were obtained by PPI network and enriched by GO and KEGG. DSS and AOM/DSS mouse models were adopted to verify the above analysis results.

Results: The enrichment analysis showed that the therapeutic targets of QCWZD enriched in blood circulation, cell adhesion molecules, and pathways of inflammation and cancer such as IL-17 signaling pathway and toll-like receptor signaling pathway were involved in the multiple synergies of QCWZD on UC and UCAC treatment. The results of experiments demonstrated that QCWZD can exert its effects on protecting the intestinal mucosal barrier, regulating inflammation and improving intestinal fibrosis in UC and UCAC and the main mechanism of QCWZD in treatment of UC and UCAC may be related to the activation of the IL-17, NF-κB and TLR4 signaling pathways.

Conclusion: Our results indicated that QCWZD treated UC and UCAC via multiple targets and pathways and the IL-17, NF-κB and TLR4 signaling pathways may be highly involved in this process.

Keywords: QCWZD, ulcerative colitis, ulcerative colitis-associated carcinogenesis, colitis-associated cancer, intestinal fibrosis

Plain Language Summary

Colitis-associated cancer (CAC) is a malignant disease of the colon caused by recurrent episodes of chronic intestinal inflammation. Qingchang wenzhong decoction (QCWZD) is an effective and classical herbal prescription for the treatment of ulcerative colitis (UC) or ulcerative colitis-associated carcinogenesis (UCAC) in clinics. QCWZD has the preponderant effect of alleviating chronic intestinal mucosa damage associated with the disease. However, the underlying mechanism is still unknown. A comprehensive strategy of

Received: 22 December 2022
Accepted: 22 February 2023
Published: 7 April 2023

genomic data mining, network pharmacology and biological verification on animals was already used to confirm that the role of QCWZD in the treatment of UC and UCAC. The results demonstrated that QCWZD can exert its effects on protecting the intestinal mucosal barrier, regulating inflammation and improving intestinal fibrosis in the treatment of UC and UCAC. The most prominent mechanism may be related to the activation of the IL-17, NF-κB, and TLR4/β-catenin/HIF-1α signaling pathways. QCWZD is a promising therapeutic strategy for UC and UCAC treatment via regulation of multiple targets and pathways, especially through alleviating inflammation and intestinal fibrosis.

Introduction

Ulcerative colitis (UC) is a group of chronic inflammatory bowel disease characterized by diarrhea and gastrointestinal bleeding.[1] The incidence and prevalence of UC have experienced rapid growth worldwide, especially in developed countries and urban areas. Numerous population-based studies have demonstrated that compared with patients with a short duration of UC, patients with a long duration of UC are at higher risk for developing ulcerative colitis-associated carcinogenesis (UCAC). Cumulative incidence of colorectal cancer (CRC) was 2% at 10 years for patients with UC, by 20 years, the incidence had widened to 8%, and even 18% at 30 years.[2] There is strong experimental and clinical evidence suggesting that chronic inflammation appears to be the main factor in promoting carcinogenesis.[1] The mechanism of CRC caused by chronic intestinal inflammation has yet to be fully unraveled. However, persistent inflammation and repeated damage and repair promote the occurrence and development of colitis-associated cancer.[3]

Qingchang Wenzhong Decoction (QCWZD) is a classic and effective prescription for the clinical treatment of UC and contains the following eight herbs: Coptis deltoidea C.Y.Cheng & P.K.Hsiao (Huanglian, HL), Zingiber officinale Roscoe (Paojiang, PJ), Sophora flavescens Aiton (Kushen, KS), Indigofera tinctoria L. (Qingdai, QD), Sanguisorba officinalis L. (Diyu, DY), Dolomiaea costus (Falc.) Kasana & A.K.Pandey (Muxiang, MX), Panax notoginseng (Burkill) F.H.Chen (Sanqi, SQ), and Glycyrrhiza glabra L. (Gancao, GC). QCWZD has already been shown to alleviate intestinal inflammation in the models of acute and chronic colitis, which is probably linked to the regulation of the interactive network of inflammation, oxidative stress, apoptosis, barrier function, and intestinal microbiota.[4,5] Meanwhile, it can accelerate intestinal mucosal repair by modulating the gut microbiota and metabolism, thereby promoting epithelial proliferation mediated by intestinal stem cells.[4] Since the ingredients of QCWZD are complex and the pharmacological mechanisms might implicate multiple signaling pathways, traditional experimental methods are not sufficient to elucidate the complex mechanism of QCWZD for preventing and treating UCAC. Given the multi-component, multi-target and synergistic characteristics of herb medicines, network pharmacology was used as a powerful tool in this study. The bioactive chemical components of QCWZD and its potential mechanisms against colitis to colitis-associated carcinogenesis (CAC) were investigated via network pharmacology analysis. Meanwhile, the mouse models of colitis and CAC were induced by dextran sulfate sodium salt (DSS) and azoxymethane (AOM) to identify the protective mechanism of QCWZD on colitis and CAC and verified the result in vivo experiment.

Materials and Methods

Bioactive Compounds Screening and Collection of Compound-Related Targets

The components of QCWZD were collected from the Traditional Chinese Medicine Systems Pharmacology (TCMSP) database (https://old.tcmsp-e.com/tcmsp.php), and the bioactive compounds were screened by oral bioavailability (OB)≥30% and drug-likeness (DL)≥0.18.[6] In parallel, some compounds with significant pharmacological effects but not screening criteria were also chosen for further studies. The compound-related targets were identified from TCMSP, Swiss Target Prediction (http://www.swisstargetprediction.ch/)[7] and Similarity Ensemble Approach (SEA, http://sea.bkslab.org/).[8]

Collection of UC-UCAC-Related Targets

The study finally screened out GSE38713[9] and GSE47908[10] datasets from the Gene Expression Omnibus (GEO) database (http://www.ncbi.nlm.nih.gov/geo), and these contain samples of normal controls, UC and UCAC. Raw microarray data (CEL files) were pre-processed and normalized by the "affy" package,[11] and then transformed using the VOOM algorithm from the "limma" package to convert counts into Gaussian distributions.[12] We mapped microarray probes to ENTREZ IDs using the corresponding annotation documents. In the case of multiple probes mapped to the

same gene symbol, the average value was taken. Next, GSE38713 and GSE47908 were combined into the UC-UCAC dataset, batch effects were removed by the "sva" package, and log2 data processing and quantile standardization were used.[13] The microarrays were divided into normal control, UC, and UCAC group in the UC-UCAC dataset. Differentially expressed genes (DEGs) were identified as those with |log2 fold change (FC)| > 1 and an adjusted *P*-value <0.05.

Construction of Network and Enrichment Analyses

Herb-component-target network of QCWZD, UC-UCAC disease target network, and shared target network of QCWZD and UC-UCAC were constructed with Cytoscape v3.8.0. The network properties of nodes (genes) were evaluated by the degree centrality (DC), betweenness centrality (BC), and proximity centrality (CC). The construction of protein-protein interaction (PPI) network with a score of genes ≥0.4 was conducted in the STRING database.[14] The Metascape database (http://metascape.org) was applied to analyze the functions of the selected targets with *P*-value cut-off of 0.05.[15] GO enrichment analysis contains biological process (BP), cell component (CC), and molecular function (MF) to explain the main biological functions of targets. The KEGG analysis was applied for pathway enrichment, and significant genes were selected (*P*-value <0.05).

Validation of QCWZD Preventing and Treating Colitis and CAC in vivo

To validate the potential mechanisms of QCWZD on UC and UCAC, dextran sodium sulfate (DSS, molecular weight: 36,000–50,000 Da, MP Biomedicals) and carcinogen azoxymethane (AOM, Sigma-Aldrich)-induced C57BL/6 mice were adopted to validate the protective effect of QCWZD on colitis and CAC.

QCWZD Preparation

QCWZD granules were purchased from the Pharmacy Department of Dongfang Hospital, Beijing University of Chinese Medicine (Beijing, China), containing Coptis chinensis Franch. (Huanglian, HL) 6g, Zingiber officinale Roscoe (Ganjiang, GJ) 9g, Dolomiaea costus (Falc.) Kasana & A.K.Pandey (Muxiang, MX) 6g, Indigofera tinctoria L. (Qingdai, QD) 3g, Sanguisorba officinalis L.(Diyu, DY) 15g, Sophora flavescens Aiton (Kushen, KS) 9g, Panax notoginseng (Burkill) F.H.Chen (Sanqi, SQ) 6g, Glycyrrhiza glabra L. (Gancao, GC) 6g. In our previous research, the major compounds of QCWZD have been identified by High Performance Liquid Chromatography (HPLC) analysis.[4]

Animals

All mice experiments in this study were approved by the Animal Ethics Committee of Beijing University of Chinese Medicine, in accordance with guidelines issued by Regulations of Beijing Laboratory Animal Management. Male C57BL/6J mice aged six to eight weeks weighing 20–22g were purchased from Beijing Weitong Lihua Experimental Animal Technology Co. Ltd. Mice were housed under standard environmental conditions, including an ambient temperature 20–24°C, 12 h/12 h light–dark cycle, and ad libitum access to food and water.

Induction of Models and Drug Administration

All mice were allowed 1 week of acclimation to the Experimental Animal Laboratory before the experiments commenced. Fifty-six male C57BL/6 mice were randomly divided into 7 groups with 8 mice per group: the control, acute colitis (AC), chronic colitis (CC), CAC, and three intervention groups of QCWZD on the above models. AC: On the 10th weeks, mice in this group were fed with a 2% DSS solution for a week. CC: Two weeks later, mice received 2% DSS in drinking water for a week, and two weeks of sterile water. This process is repeated three times. CAC: mice were induced by single intraperitoneal (i.p.) injection of 10mg/kg AOM. After 1 week, mice were provided 2% DSS in drinking water for a week, sterile water for 2 weeks, and this process repeated three times.[16] For CC and CAC models, intragastric administration of QCWZD (9.25g/kg) or equivalent sterile water was conducted once a day for ten weeks. In the AC model, QCWZD or equivalent sterile water was conducted once a day for one week starting from the tenth week. Body weight was monitored weekly, mice were sacrificed at the end of the experiment, and colons were isolated for the length measurement. The mouse colon was subsequently dissected longitudinally and washed with ice-cold phosphate-buffered saline (PBS, pH 7.4, 4°C). The number of tumors was recorded through gross histopathologic examination of

the colon. Then, the colon was cut into small pieces and a portion was fixed with 4% paraformaldehyde. The remainder of the colon that was snap frozen in liquid nitrogen and stored at −80°C was used for PCR and Elisa analysis.

Disease Activity Index Analysis

All mice were monitored daily for clinical signs of colitis, including weight loss, stool consistency, and rectal bleeding. The following parameters are the bases of the measurement: 1) weight loss (0, less than 1%; 1, 1–5%; 2, 5–10%; 3, 10–15%; 4, >15%), 2) stool consistency (0, normal; 2, mushy; 4, diarrhea), and 3) rectal bleeding (0, negative; 2, positive; 4, visible rectal bleeding). The disease activity index (DAI) was calculated according to a standard scoring system.[17]

Histological Analysis

Tissues were fixed in 4% paraformaldehyde at 4°C and embedded in paraffin. Paraffin sections (5 μm) were cut and stained with hematoxylin and eosin (H&E), alcian blue/periodic acid Schiff (AB/PAS), sirius red and masson's trichrome using standard protocols. H&E slides were scored blindly by percent of the involved tissue, inflammation and regeneration, crypt damage and layers that were affected.[18]

Immunohistochemistry

Paraffin sections were dewaxed in xylene and rehydrated. Antigen retrieval was performed in a microwave by 20 min of boiling in citrate buffer (10 mmol/L, pH = 6.0). The slides were then transferred to a humid tray and incubated with 5% normal goat serum in PBS at room temperature for 1 h. The primary antibodies used in the present study included IL-17A (NBP1-76337, Novus Biologicals), IL-22 (NB100-737, Novus Biologicals), HIF-1α (NB100-479, Novus Biologicals), VEGF (NB100-664, Novus Biologicals), CD31 (3528S, Cell Signaling), ZO-1 (NBP1-85047, Novus Biologicals), Claudin-1 (NBP2-38578, Novus Biologicals), MMP9 (NBP2-13173, Novus Biologicals), and α-SMA (19245S, Cell Signaling). The sections were incubated overnight in the respective primary antibodies and blocking solution at 4°C. The slides were incubated with secondary goat anti-rabbit IgG-biotin (B8895; Sigma-Aldrich, St. Louis, MO, United States) for 1 h. The sections were incubated for 30 min using the ABC-peroxidase solution (UltrasensitiveTM S-P kit, kit 9719; Maixin-Bio, China) and counterstained with hematoxylin. The quantification of IHC was processed using the image-Pro Plus 6.0 software (Media Cybernetics, USA).

Real-Time PCR

Total RNA was extracted using a reagent kit (Tiangen Biochemical Technology, DP424, Beijing, CHINA) and subjected to reverse transcription and qPCR quantitation following the instructions. Sequences of primers used in this study are listed in Table 1. The real-time PCR conditions: 95°C for 30s, followed by 40 cycles at 95°C for 4s, 60°C for 40s and 95°C for 5 min. The threshold cycle (Ct, which is the inflection point on the amplification power curve) values were calculated using the delta-delta Ct method, and relative expression was normalized to β-actin. Five samples from each group were randomly selected to perform the RT-PCR analyses. Five samples from each group were randomly selected for RT-PCR.

Enzyme-Linked Immunosorbent Assay (ELISA)

Frozen fragments of colon tissue were weighed and homogenized with tissue extraction reagent on ice for 3 min. TNF-α, MPO, and calprotectin (CALP) were measured using mouse ELISA kits (Shanghai Enzyme-linked Biotechnology Co., Ltd., China). Five samples from each group were randomly selected to perform the ELISA analyses.

Statistical Analysis

Shapiro–Wilk test was used to assess data distribution. SPSS 20.0 statistical software was chosen to perform statistical analysis. The data of normal distribution were shown as the mean ± standard deviation (SD). The statistical significance for multiple comparisons was determined by carrying out analysis of variance (ANOVA) and Dunnett's T3 tests. Under the assumption of equal variances between groups, the least significant difference (LSD) test was performed. When the data were abnormally distributed, the median and interquartile range (IQR) were commonly used. Kruskal–Wallis H(K) test and Nemenyi test (R, PMCMRplus) were chosen to determine statistical significance for multiple comparisons. Statistical significance differences were established at $P < 0.05$, $P < 0.01$ or $P < 0.001$.

Table 1 Primer Sequences of RT-qPCR

Primer Name		Primer Sequence (5'to3')
IL-1β	Forward (5′ to 3′)	AAAAGCCTCGTGCTGTCGGA
	Reverse (5′ to 3′)	TGTCGTTGCTTGGTTCTCCTTGT
IL-17A	Forward (5′ to 3′)	ACCCTGATAGATATCCCTCTGTGA
	Reverse (5′ to 3′)	GCTTTCCCTCCGCATTGA
IL-22	Forward (5′ to 3′)	GGTGACGACCAGAACATCCA
	Reverse (5′ to 3′)	CAGCAGGTCCAGTTCCCCAAT
IL-10	Forward (5′ to 3′)	ACTCCTTGGAAAACCTCG
	Reverse (5′ to 3′)	AAGAACCCCTCCCATCAT
HIF-1α	Forward (5′ to 3′)	AAGGACAAGTCACCACAGGACA
	Reverse (5′ to 3′)	AGGGAGAAAATCAAGTCGTGCT
TLR4	Forward (5′ to 3′)	AGAATGAGGACTGGGTGAGAAATGA
	Reverse (5′ to 3′)	CAATGAAGATGATGCCAGAGCG
NF-κB	Forward (5′ to 3′)	TGCTGTGCCTACCCGAAACTC
	Reverse (5′ to 3′)	GTTGATGGTGCTGAGGGATGCT
β-catenin	Forward (5′ to 3′)	GCTTCTGGGTTCCGATGATA
	Reverse (5′ to 3′)	CACTTGGCACACCATCATCTT
REG-3γ	Forward (5′ to 3′)	CGACACTGGGCTATGAAC
	Reverse (5′ to 3′)	GTGATTGCCTGAGGAAGA
MUC-2	Forward (5′ to 3′)	GCTCCGGCATCATCGTTA
	Reverse (5′ to 3′)	GTCTGGGTTGTGGCTTAC
β-Actin	Forward (5′ to 3′)	CGTTGACATCCGTAAAGACCTC
	Reverse (5′ to 3′)	ACAGAGTACTTGCGCTCAGGAG

Results

Herb-Compound-Target Network of QCWZD

A total of 208 active chemical ingredients in QCWZD after deduplication were identified from the TCMSP database. Twenty-seven active ingredients emerged from the "monarch herbs" (HL, GJ), 73 active compounds derived from the "minister herbs" (DY, KS and QD), 42 active components come from the "adjuvant herbs" (SQ, MX) and 92 active components stem from the "guide herbs" (GC) (Figure 1A). In total, 800 chemical ingredient-related targets in QCWZD were confirmed. There are 125 "monarch-herb" targets, 76 "minister-herb" targets, 268 "adjuvant-herb" targets and 21 "guide-herb" targets were unique in QCWZD. Apart from that, there were 12 targets that the "monarch-herb" and "minister-herb" have in common. Three targets were assumed to be shared among the "monarch-herb" and the "adjuvant and guide-herb". One hundred and seventeen targets were common to 2 regions of "minister-herb" and "adjuvant and guide-herb". In summary, 81 ingredient-related targets were overlapped among all three kinds of herbs (Figure 1B).

To further clarify the link between the herbs, active ingredients and underlying targets, the herb- ingredient-target network of QCWZD was built, as shown in Figure 1C. The network consisted of 1033 nodes and 3069 edges. Moupinamide, quercetin, lauric acid, adenosine, kaempferol, saussureamine B, Gallic acid, naringenin, luteolin and

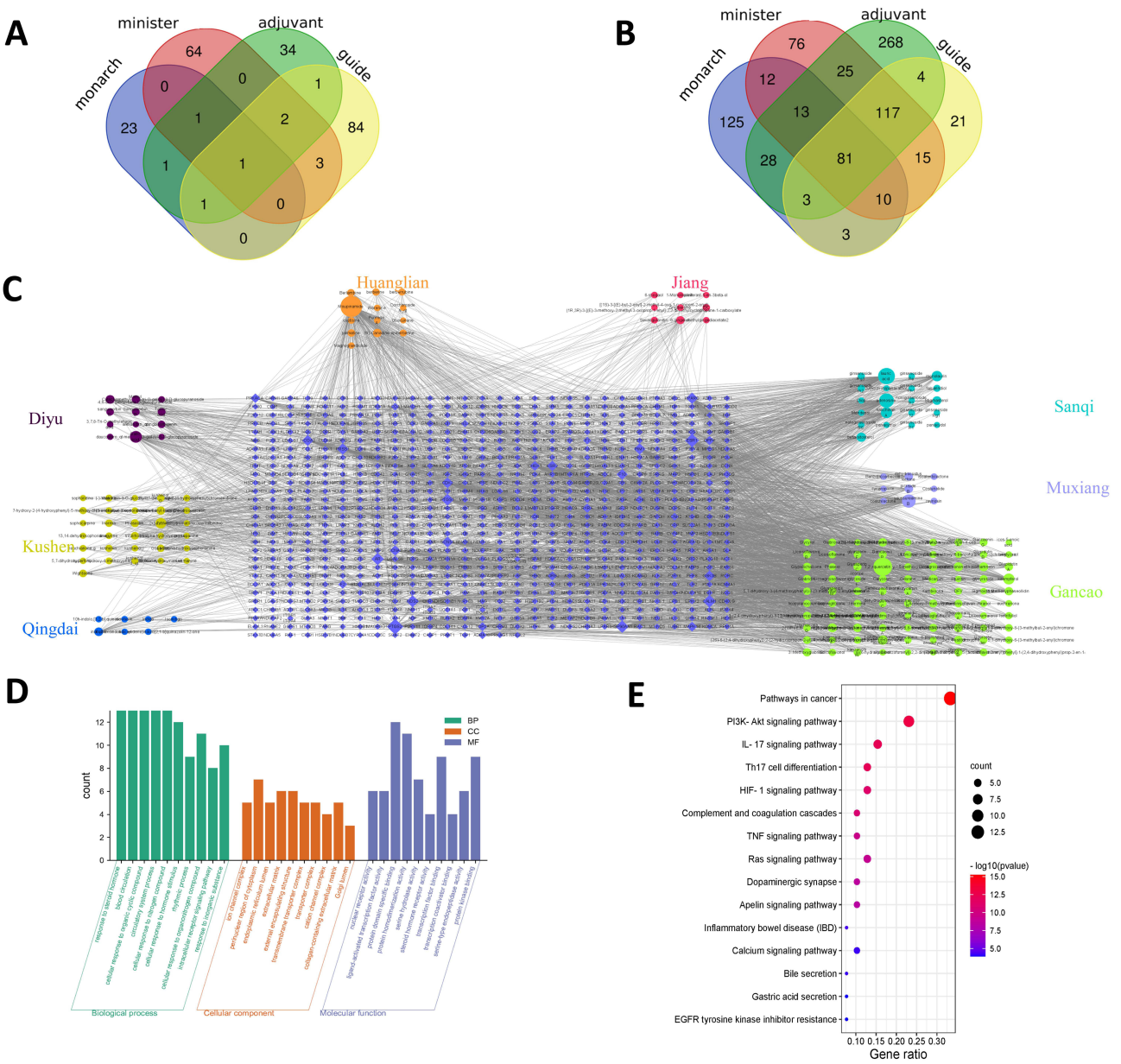

Figure 1 QCWZD-related targets network and analysis.(**A**) Distribution of ingredients among the herbs; (**B**) Distribution of targets among the herbs; (**C**) QCWZD-related targets network; (**D**) GO enrichment analysis for QCWZD-related targets; (**E**) KEGG enrichment analysis for QCWZD-related targets.

sanchinan A were predicted as the critical active ingredients of QCWZD in accordance with the degree and betweenness centrality by topological analysis. In addition, PTGS2, PTGS1, ESR1, CALM1, HSP90AA1, POLB, PRKACA, ADRB2, PPARG, and RELA were the main targets of QCWZD based on degree and betweenness centrality.

In order to further analyze the signature of QCWZD-related targets, we performed GO and KEGG pathway enrichment analyses. GO analysis demonstrated that the majority of targets were involved in the regulation of transcription, signal transduction, and response to the drug. These observations suggested the multiple synergistic effects of QCWZD on biological processes (Figure 1D). In addition, KEGG results revealed that QCWZD-related targets were significantly enriched in 29 pathways. The top 15 enriched pathways involved in Pathways in cancer, PI3K-Akt signaling pathway, IL-17 signaling pathway, Th17 cell differentiation, HIF-1 signaling pathway, Complement and coagulation cascades, TNF signaling pathway, Ras signaling pathway, Dopaminergic synapse, Apelin signaling pathway,

Inflammatory bowel disease (IBD), Calcium signaling pathway, Bile secretion, Gastric acid secretion, and EGFR tyrosine kinase inhibitor resistance (Figure 1E).

Shared Targets Between QCWZD Targets and UC-UCAC Targets

The workflow of gene extraction and creation pipeline is displayed in Figure 2A. After pre-processing and removing outliers from the primary UC-datasets, a total number of 284 differential genes (DEGs) were pinpointed as the UC-UCAC targets (Figure 2B). Subsequent analysis revealed that 32 targets were shared between 800 QCWZD targets and 284 UC-UCAC targets (Figure 2C). Thirty-two overlapping targets were with high confidence scores (confidence score ≥0.4) in accordance with PPIs performed from the STRING database, recommending their highly significant associations (Figure 2D). Then, the herb-compound-overlapping target network of QCWZD was established, as found in Figure 2E.

Overlapping Targets Network

Central network evaluation was performed to acquire key targets. Finally, 29 key targets with 69 interactions were obtained in the overlapping targets network (Figure 3A). Topology analysis indicated that IL-1β, CXCL8, MMP9, PTGS2, SELE, MMP1, MMP3, PPARG, CAV1, and CXCL11were the top 10 targets based on the CytoHubba plug-in MCC algorithm (Figure 3B).

GO enrichment analysis results after initial screening are revealed in Figure 3C. The BP of 32 genes was primarily enriched in blood circulation, the response to steroid hormone, cellular response to organic cyclic compound, circulatory system process, cellular response to nitrogen compound, cellular response to the hormone stimulus, rhythmic process, cellular response to organonitrogen compound, intracellular receptor signaling pathway, and response to inorganic

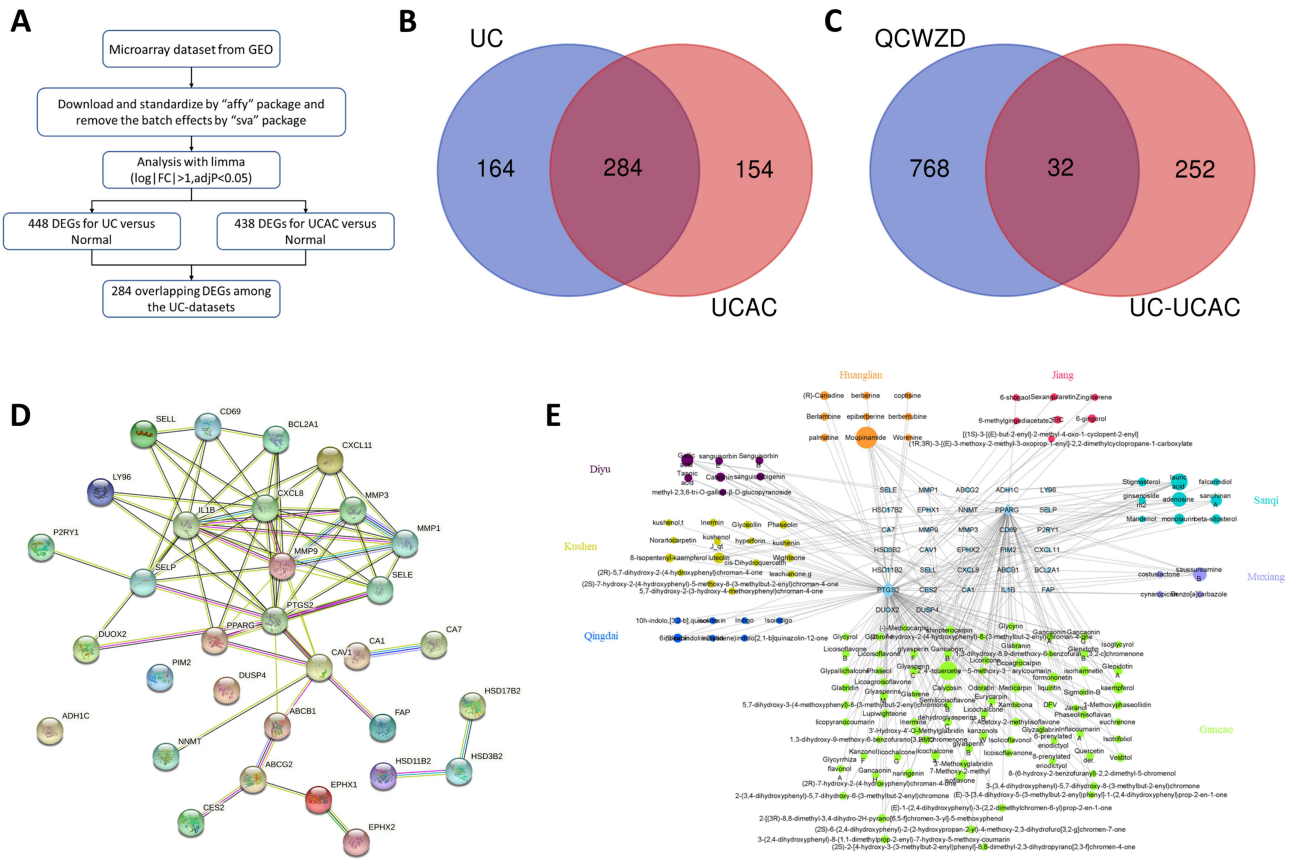

Figure 2 Shared targets between QCWZD targets and UC-UCAC targets. (**A**) Workflow of gene extraction and creation process; (**B**) 284 overlapping targets for UC and UCAC; (**C**) 32 targets between QCWZD and UC-UCAC targets; (**D**). PPI for 32 overlapping targets Network diagram; (**E**) The herb-compound-overlapping target network of QCWZD.

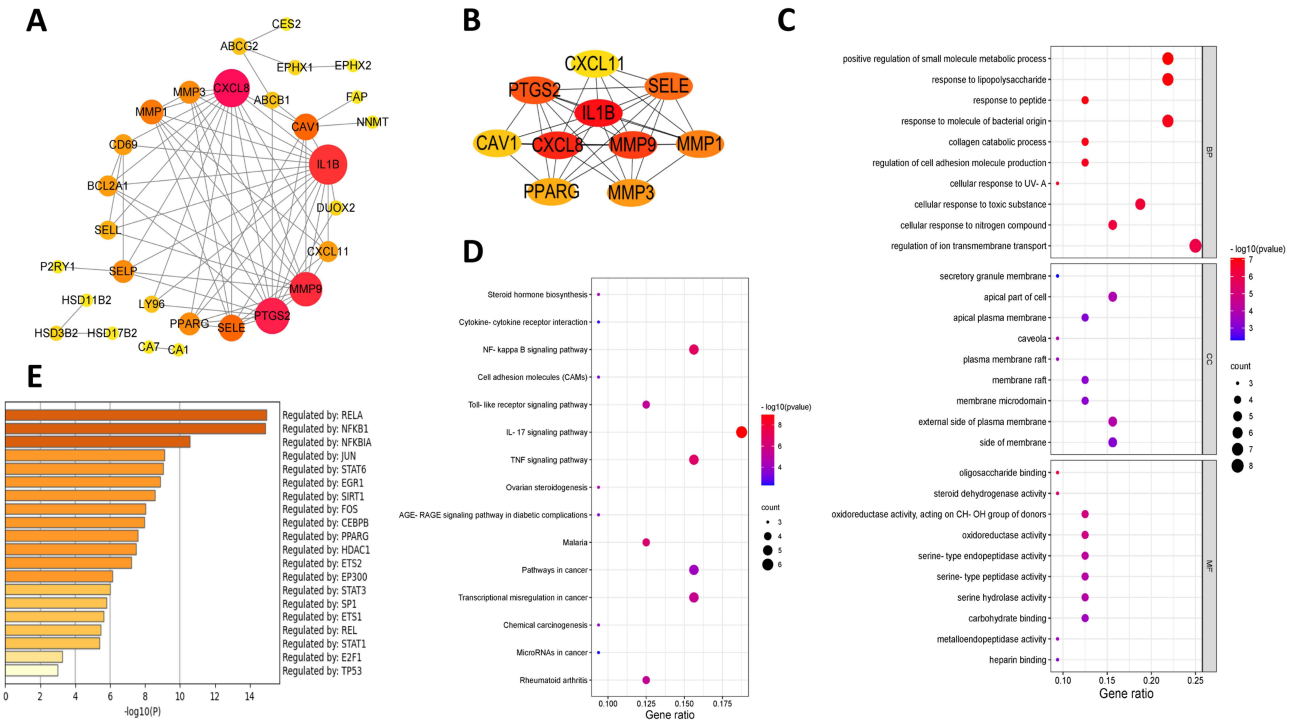

Figure 3 Overlapping targets network. (**A**) 29 key targets in the overlapping targets network; (**B**) The top 10 targets based on the CytoHubba plug-in MCC algorithm; (**C**) GO enrichment analysis; (**D**) KEGG pathway analysis; (**E**) Predicted that transcription factors.

substance. The CC analysis results demonstrated that the genes are mainly involved in ion channel complex, perinuclear region of cytoplasm, endoplasmic reticulum lumen, extracellular matrix, external encapsulating structure, transmembrane transporter complex, transporter complex, cation channel complex, collagen-containing extracellular matrix, and Golgi lumen. The MF analysis suggested that these genes were enriched in nuclear receptor activity, ligand-activated transcription factor activity, protein domain-specific binding, protein homodimerization activity, serine hydrolase activity, steroid hormone receptor activity, transcription factor binding, transcription coactivator binding, and serine-type endopeptidase activity. KEGG pathway analysis showed the enrichment in steroid hormone biosynthesis, Cytokine–cytokine receptor interaction, NF-κB signaling pathway, Cell adhesion molecules (CAMs), Toll-like receptor signaling pathway, IL-17 signaling pathway, TNF signaling pathway, ovarian steroidogenesis, AGE-RAGE signaling pathway in diabetic complications, malaria, pathways in cancer, transcriptional misregulation in cancer, chemical carcinogenesis, microRNAs in cancer, and rheumatoid arthritis (Figure 3D). Simultaneously, it predicted that transcription factors (RELA, NFKB1, NFKBIA, JUN, STAT6, EGR1, STAT1, et al) may regulate the expression of these genes (Figure 3E).

QCWZD Alleviates Signs and Symptoms of DSS and AOM/DSS Mice

The previous research has confirmed that the major components of QCWZD were stable and repeatable by the high-performance liquid chromatography (HPLC) analysis.[4] The network pharmacological results showed that blood circulation, cell adhesion molecules, and pathways of inflammation and cancer such as toll-like receptor signaling pathway and IL-17 signaling pathway were involved in the multiple synergies of QCWZD on UC and UCAC treatment.

To illustrate the therapeutic effect of QCWZD and its effects on the transition from inflammation to cancer, the models (acute colitis, chronic colitis and CAC) were established, respectively (Figure 4A). Compared to mice in AC and CAC groups, the mice that received QCWZD treatment displayed a markedly faster intestinal restoration process that could be observed by the increased body weight gain and a lower DAI (Figure 4B and C; Supplementary Tables 1 and 2). Furthermore, macroscopic analysis detected colon length in the mice group of QCWZD treatment was longer than that in the model groups ($P < 0.001$, Figure 4D and E). As expected, several colonic tumors were seen in all CAC mice. QCWZD treatment obviously reduced the incidence and size of tumors ($P < 0.05$, Figure 4F and G). Consequently, mean tumor load, defined as the sum of diameters of all

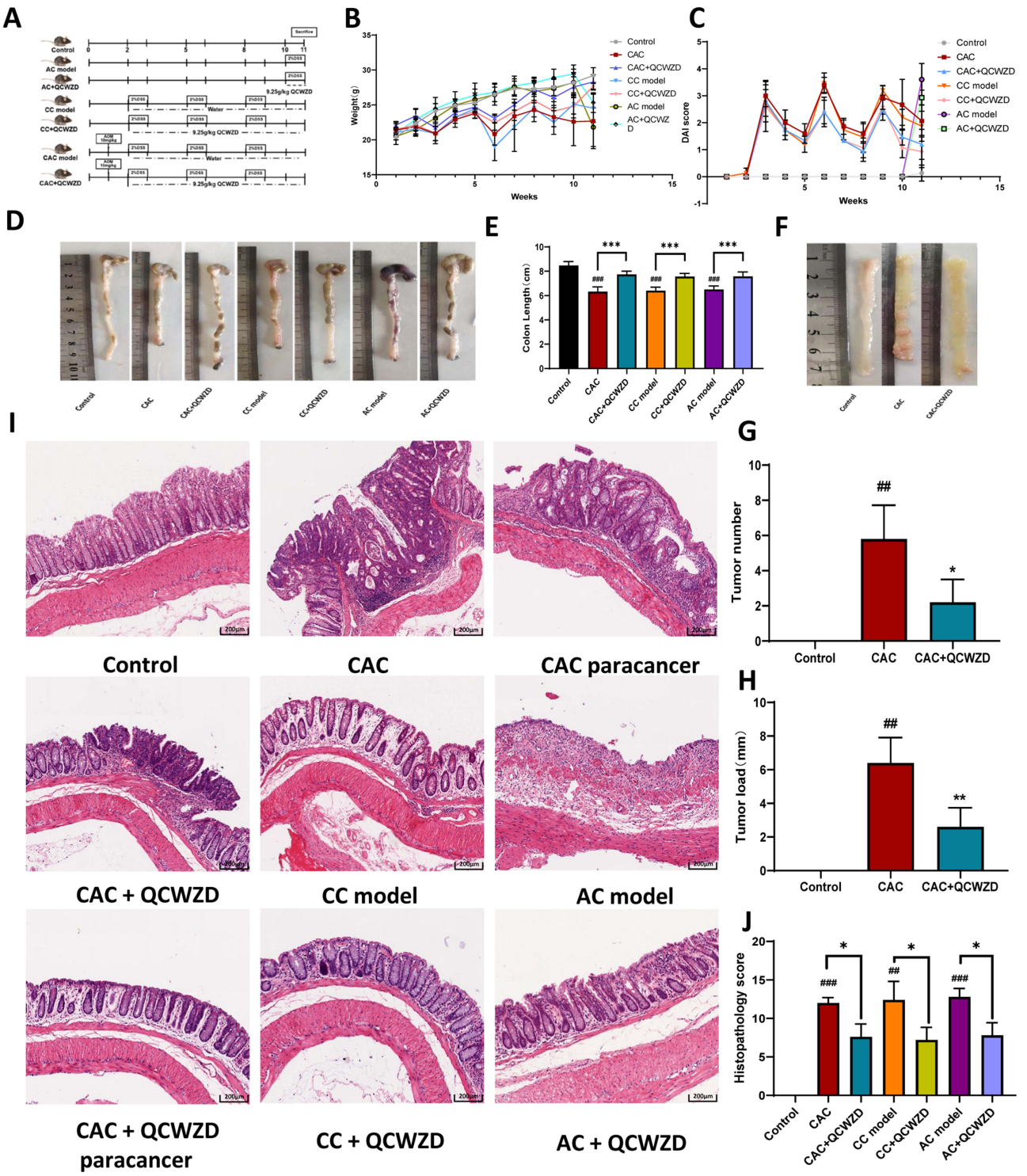

Figure 4 Pharmacodynamic validation of QCWZD in animals: (**A**) Schematic overview of control, AC, CC and CAC model; (**B**) different groups of small Changes in body weight of mice; (**C**) Changes in disease activity index (DAI) of mice in different groups; (**D** and **E**) Colon lengths of mice in each group at 11 weeks; (**F** and **G**) The number of tumors in CAC and administration group; (**H**) The size of tumors in CAC and administration group; (**I**) H&E staining of sections; (**J**) Histopathological score. *P < 0.05, **P < 0.01, ***P < 0.001; ###P < 0.01, ####P < 0.001 vs control.

Abbreviations: AC, acute colitis; CC, chronic colitis; CAC, colitis-associated cancer; QCWZD, Qingchang wenzhong decoction; ns, not significant.

tumors in a certain mouse, was shrunk in the QCWZD group (Figure 4H) ($P < 0.01$). Histologic evaluation indicated colon crypts and mucosal damage in the AC model, crypt atrophy and abnormal epithelial in the CC model, and mucosal structure disorder in the CAC model induced by AOM/DSS. Moreover, QCWZD could decrease inflammatory infiltrate and crypt abscesses, restore

mucosal structure and inhibit the transition from inflammation to cancer. These issues revealed that QCWZD has a pronounced inhibitory effect on DSS-induced colitis and AOM/DSS-induced colorectal tumorigenesis ($P<0.05$, Figure 4I and J).

QCWZD Improves the Intestinal Epithelial Barrier Structure and Function in DSS and AOM/DSS Mice

AB/PAS staining pointed out that the DSS and AOM/DSS-induced mice performed awfully decreased colonic goblet cells, while QCWZD could supplement the goblet cells, which is pivotal for the preservation of gut homeostasis (Figure 5A). To further investigate the mechanism of the intestinal epithelial barrier repair by QCWZD treatment, we examined the levels of tight junction-associated proteins Claudin-1 and ZO-1. Immunohistochemistry analysis revealed dramatically increased expression patterns of Claudin-1 and ZO-1 in colonic epithelial cells purified from QCWZD-treated AC, CC and CAC mice compared with the levels of DSS and AOM/DSS-induced mice (Figure 5B and C). Meanwhile, antimicrobial peptides (AMPs) are multifunctional molecules important for host defense and play important roles in fighting microbe pathogens, and the mRNA expression level of REG-3γ and MUC2 from RT-qPCR was enhanced in QCWZD-treated DSS and AOM/DSS mice (Figure 5D).

QCWZD Regulates Immune Responses in DSS and AOM/DSS Mice

To study the possibility that QCWZD improves the intestinal injury and malignant transformation of colitis via modulating enteric mucosal immune responses, we assessed the expression level of colonic inflammation-related indicators of DSS and AOM/DSS mice treated with QCWZD. The results of immunohistochemistry showed that the proinflammatory cytokine IL-17A was higher in DSS and AOM/DSS-induced models than those in the control group, and QCWZD inhibited the expression of IL-17A. Interestingly, QCWZD promoted the expression of IL-22 in the AC and CC model to protect the intestinal mucosa, but QCWZD decreased the level of IL-22 in the CAC

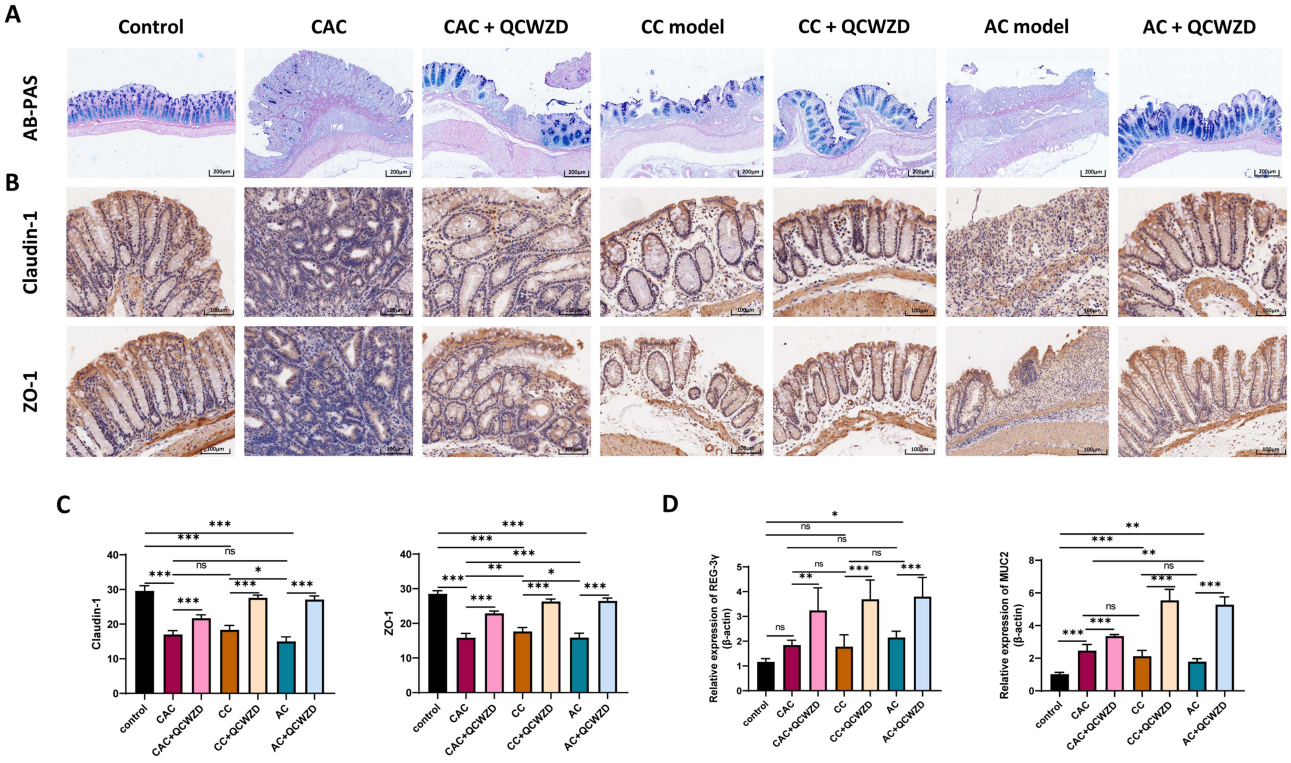

Figure 5 QCWZD improves intestinal epithelial barrier structure and function in DSS and AOM/DSS mice. (**A**) AB/PAS staining of goblet cells; (**B**) Immunohistochemical of Claudin-1 and ZO-1 in colon tissue; (**C**) Semi-quantitative immunohistochemical analysis of Claudin-1 and ZO-1; (**D**) The mRNA expression levels of REG-3γ and MUC2 in each group. *P < 0.05, **P < 0.01, ***P < 0.001.

Abbreviations: AC, acute colitis; CC, chronic colitis; CAC, colitis-associated cancer; QCWZD, Qingchang wenzhong decoction; ns, not significant.

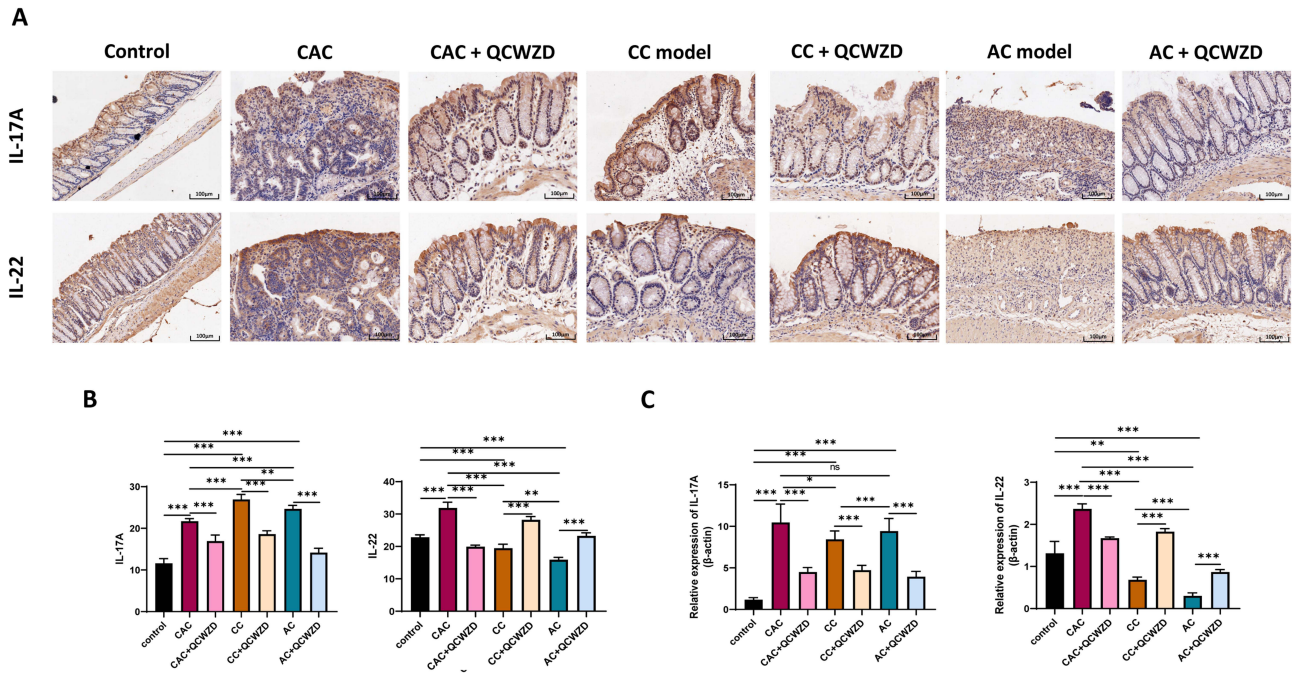

Figure 6 QCWZD regulates IL-17A and IL-22 in DSS and AOM/DSS mice. (**A**) Immunohistochemical of IL-17A and IL-22 in the colon tissue; (**B**) Semi-quantitative immunohistochemical analysis of IL-17A and IL-22; (**C**) The mRNA expressions of IL-17A and IL-22 in the colon. *P < 0.05, **P < 0.01, ***P < 0.001.
Abbreviations: AC, acute colitis; CC, chronic colitis; CAC, colitis-associated cancer; QCWZD, Qingchang wenzhong decoction; ns, not significant.

model and reversed this trend (Figure 6A and B). The mRNA of IL-17A and IL-22 was similar to the trend of those in immunohistochemistry (Figure 6C). Network pharmacology analysis indicates that the underlying pathways of QCWZD in the treatment of UC and UCAC were significantly enriched in the toll-like receptor signaling pathway and IL-17 signaling pathway. As shown in Figure 7A1–A3, the mRNA expression of TLR4, NF-κB, and β-catenin in colon were determined by qRT-PCR, and QCWZD supplementation inhibited the expression of these indicators. The same trend appeared for the mRNA of IL-1β in Figure 7B1. Furthermore, we found that the expression trend of IL-10 was different from that of IL-22, and IL-10 played a key role in inhibiting colitis carcinogenesis even in the CAC model (Figure 7B2). Concurrently, ELISA results also demonstrated that QCWZD intervention significantly curbed the level expressions of TNF-α, MPO and CALP in the colonic mucosal (Figure 7C1–C3).

QCWZD Attenuates Inflammation-Induced Intestinal Fibrosis

Inflammation is a known primary process that causes fibrosis in the colon. We analyzed collagen deposition by Masson trichrome and Sirius red staining to examine whether QCWZD affects fibrosis in the DSS and AOM-DSS model. Both stains indicated increased areas of fibrosis/collagen deposits in CC and CAC mice colons compared to colons from the control mice, which decreased after treatment with QCWZD, suggesting that intestinal fibrosis is affected by QCWZD (Figure 8A). Extracellular matrix (ECM) performs a crucial role in cancer metastasis, linking the transition from inflammation to cancer. As depicted in Figure 8B and C, a significant up-regulation of α-SMA and MMP9 were observed in CC and CAC mice in comparison with the control group, indicating the occurrence of epithelial-mesenchymal transition (EMT) in the DSS and AOM/DSS model group. QCWZD treatment was found to dramatically decrease the expression levels of the above indicators. Concurrently, the angiogenic switch is a hallmark of tumor progression, and is an essential means by which tumor growth in the colon is supported. HIF-1α is a central mediator regulating the expression of genes that promote tissue oxygenation and vascularization, such as VEGF, and CD31. When cellular oxygen declines, HIF-1α is activated and increases the transcription of its downstream targets.[19] Immunohistochemical results showed that the levels of HIF-1α, VEGF and CD31 were significantly elevated in CC and CAC models, while

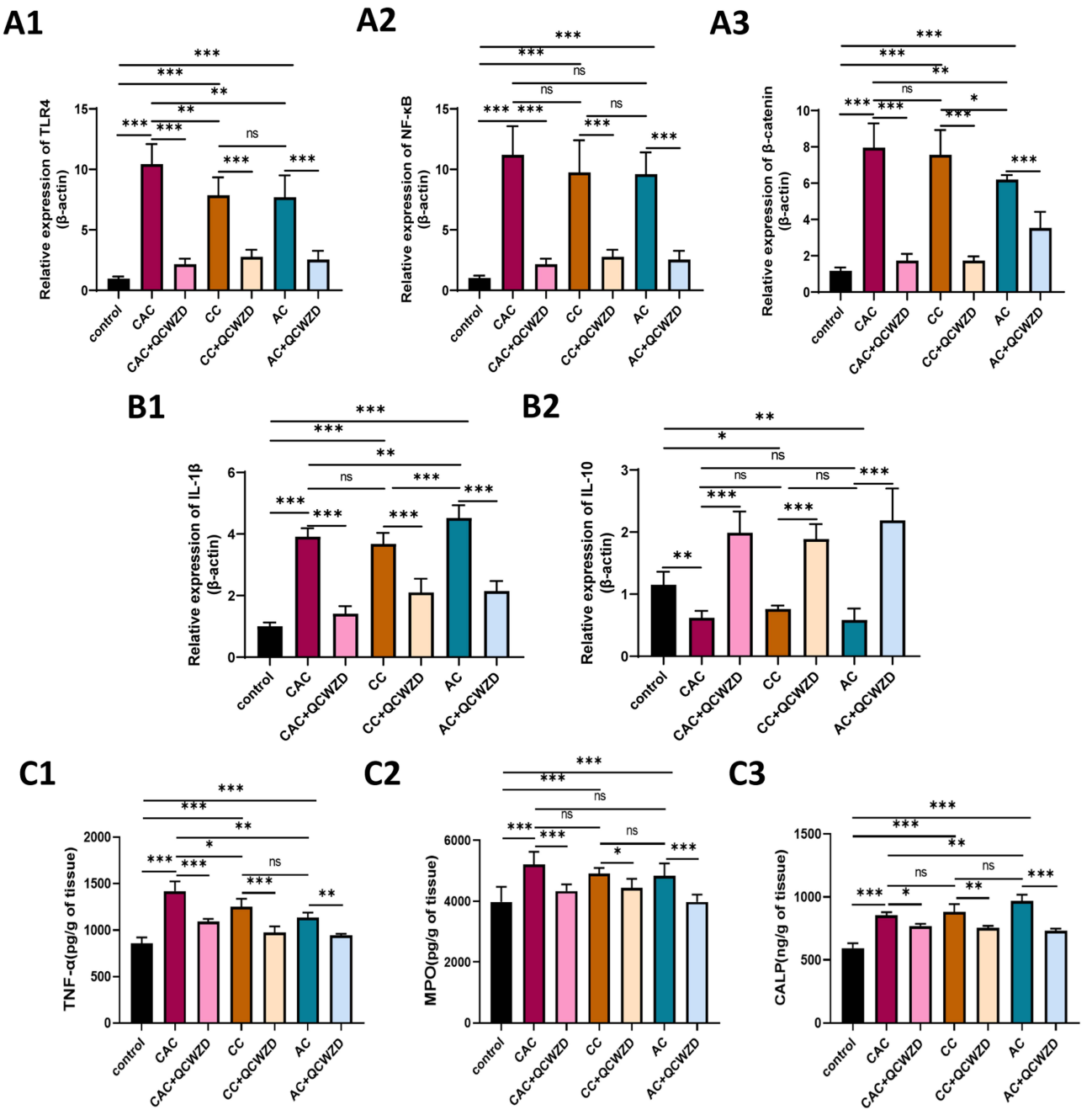

Figure 7 QCWZD modulates immune responses in DSS and AOM/DSS mice. (**A**) The mRNA expressions of TLR4 (**A1**), NF-Kb (**A2**) and β-catenin (**A3**) in the colon; (**B**) The mRNA expressions of IL-1β (**B1**) and IL-10 (**B2**) in the colon; (**C**) ELISA Protein expression of TNF-α (**C1**), MPO (**C2**) and CALP (**C3**) by Elisa in colon. *P < 0.05, **P < 0.01, ***P < 0.001.

Abbreviations: AC, acute colitis; CC, chronic colitis; CAC, colitis-associated cancer; QCWZD, Qingchang wenzhong decoction; ns, not significant.

QCWZD suppressed their expression (Figure 9A and B). Meanwhile, the mRNA levels of HIF-1α also confirmed this trend (Figure 9C).

Discussion

In the present study, 284 UC-UCAC-related targets were identified from datasets GSE38713 and GSE47908. In total, 208 active compounds and 800 compound-related targets of QCWZD were compiled from public databases. Among these known targets, 32 targets were shared between compound-related and UC-UCAC-related targets, implicating that

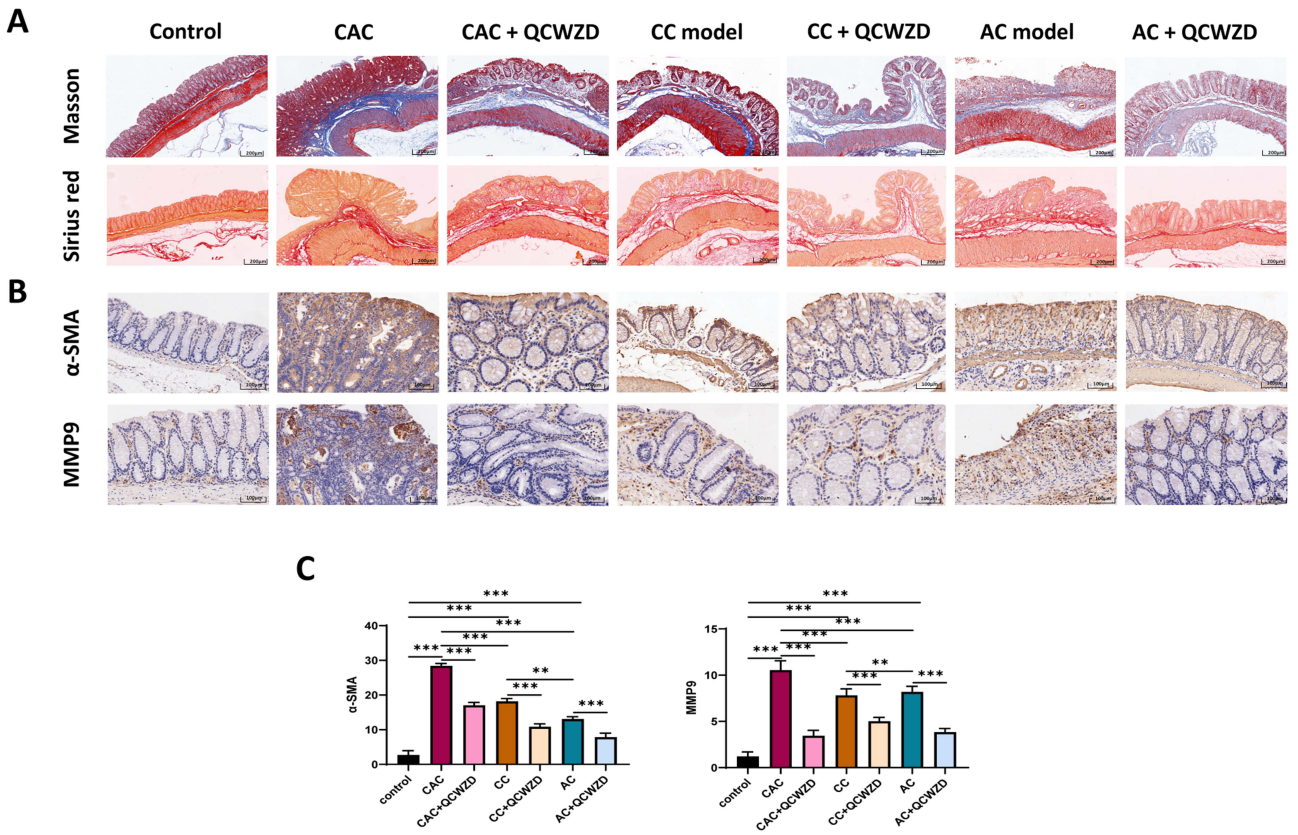

Figure 8 QCWZD attenuates inflammation-induced intestinal fibrosis. (**A**) Intestinal fibrosis detected by Masson trichrome and Sirius red staining; (**B**) α-SMA and MMP9 expression in immunohistochemistry; (**C**) Semi-quantitative immunohistochemical analysis of α-SMA and MMP9. **P < 0.01, ***P < 0.001.
Abbreviations: AC, acute colitis; CC, chronic colitis; CAC, colitis-associated cancer; QCWZD, Qingchang wenzhong decoction.

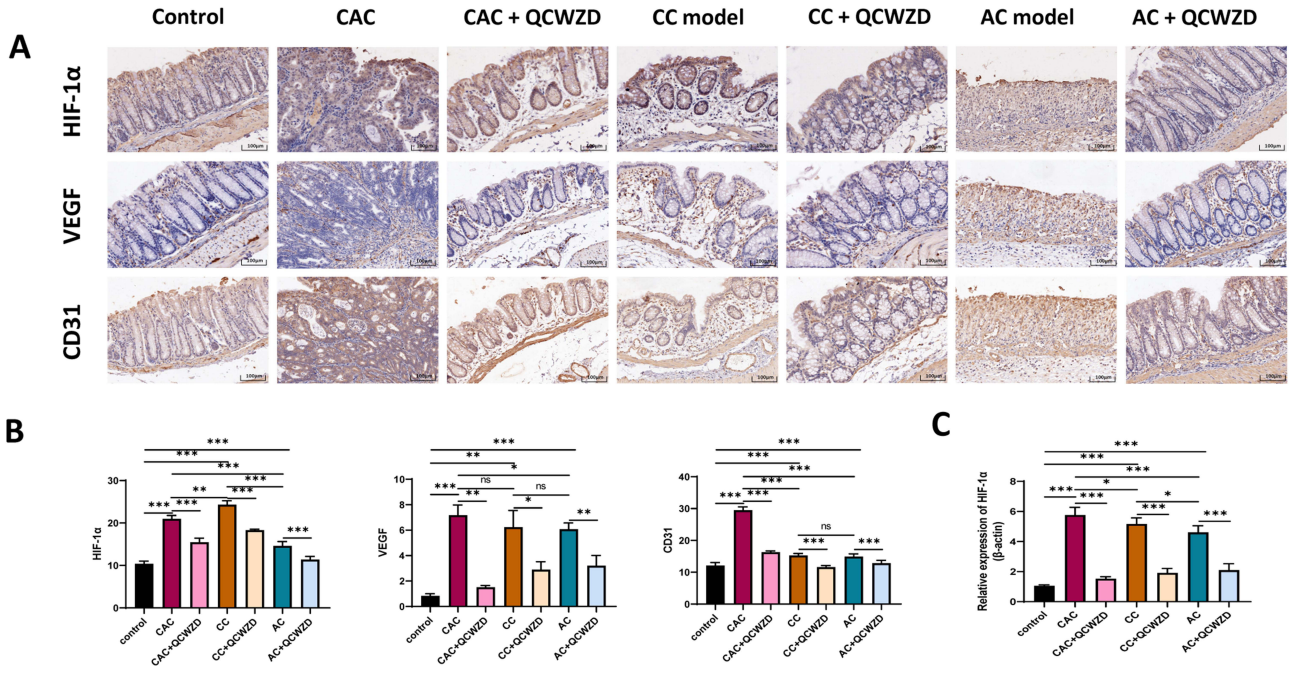

Figure 9 QCWZD attenuates angiogenesis in DSS and AOM/DSS mice. (**A**) HIF-1α, VEGF and CD31 expression in immunohistochemistry; (**B**) Semi-quantitative immunohistochemical analysis of HIF-1α, VEGF and CD31; (**C**) The mRNA expression level of HIF-1α in colon. *P < 0.05, **P < 0.01, ***P < 0.001.
Abbreviations: AC, acute colitis; CC, chronic colitis; CAC, colitis-associated cancer; QCWZD, Qingchang wenzhong decoction; ns, not significant.

QCWZD may have a therapeutic effect on UC carcinogenesis. From the key targets and enrichment analysis, it can be found that QCWZD may play a role in inhibiting the carcinogenesis of colitis through related pathways such as inflammation and cancer-related pathways and epithelial-mesenchymal transition. Our findings provide comprehensive insight into the multi-target mechanisms of QCWZD in the treatment of UC-UCAC for the first time, which might present experimental justification for the therapeutic application of QCWZD in UC-UCAC treatment.

TCM formulae are grounded in the traditional planning principles of "Jun-Chen-Zuo-Shi", which means monarch, minister, adjuvant and guide drugs, respectively. In QCWZD, the "monarch herbs" contain HL and PJ. The "minister herbs" are composed of DY, KS, and QD. SQ and MX play the role of "adjuvant herb", and GC constitutes the "guide herb". In this study, 125, 76, 268 and 21 compounds were identified from the "monarch herbs", "minister herbs", "adjuvant herb", and "guide herb", respectively. These detailed pharmacological shreds of evidence might support QCWZD to be defined as multi-target drugs in treating UC-UCAC. In fact, some components in QCWZD have been reported to show biological activities in the treatment of UC as well as colorectal cancer. Duan et al summarized related studies that berberine, quercetin, naringenin, luteolin, and kaempferol can significantly reduce DSS-induced weight loss, colon shortening, and colon damage.[20] The protective effect of Indigo Naturalis in DSS-induced colitis was also confirmed in our previous study.[21] Moreover, Berberine and quercetin treatment suppresses the viability of colorectal cancer cells by increasing their apoptosis level.[22,23] Kaempferol suppressed glycolysis and colon cancer growth by regulating the miR-339-5p-hnRNPA1/PTBP1-PKM2 axis.[24] Gallic acid inhibited tumor growth, promoted tumor apoptosis and reduced the level of p-SRC, p-EGFR, p-STAT3 and p-AKT.[25]

CAC is predisposed to long-term exposure to chronic inflammation in IBD patients.[26] IL-17A levels are elevated in serum and colon mucosa of IBD patients.[27] AOM/DSS-induced IL-17A knockout mice show decreased tumor growth and/or development.[28] Some studies also show that there is a significantly increased number of Th17 cells in CRC tissues.[29,30] Xie et al found that the extracellular receptor kinase (ERK)1/2 signaling pathway could be activated by IL-17, and increase the expression of IL-17 downstream genes such as MMP-9, and MMP-7.[31] Furthermore, NF-κB is involved in tumor promotion, proliferation, angiogenesis and metastasis by transcriptional regulation of a wide spectrum of genes.[32,33] Numasaki et al found higher vascular density in models of fibrosarcoma and colon adenocarcinoma transduced with IL-17.[34] IL-17 can promote CRC angiogenesis via binding to the IL-17 receptor (IL-17R) and stimulating endothelial cell expression to produce VEGF.[35] In contrast to IL-17A, IL-22 contributes to mucosal protection against pathogens and tissue repair in inflammatory settings.[36] However, it can directly enhance the proliferative and survival of epithelial cells, IL-22 is highly expressed in colon cancer and promoted cancer progression.[37]

In particular, there is a growing body of indirect evidence that has indicated that the TLR4-mediated signaling could contribute to pathogen-activated tumor signal pathway and play a pivotal role involved in the CAC development.[38] TLR4 is a typical inflammatory mediator and has emerged as a bridge between innate and adaptive immunity, as well as between infection and inflammation.[39] According to some studies, the TLR4/MD2 expression levels on intestinal epithelial cells are fairly low or absent in normal conditions, but dramatically upregulated in the course of IBD development.[40] Moreover, disturbance of the TLR4 pathway has been regarded as one of the unique aspects of IBD-related tumor.[41] Importantly, Fukata et al[42] confirmed that the epithelial TLR4 expression was gradually increased from the primary lesions of active UC to those of low-grade dysplasia, high-grade dysplasia and CAC in clinical samples.[43] This is consistent with our findings and that QCWZD can reduce the mRNA expression level of TLR4. In several cancers, constitutive nuclear β-catenin expression and overactivated Wnt/β-catenin signaling have been reported, including CRC, where growth, invasion, and metastasis in cancer were promoted by them.[44] With colorectal cancer (CRC), a mutation(s) in the Wnt/β-catenin pathway have (has) been detected in 90% of all tumors. Due to the essential role NF-κB and Wnt signaling play in CRC, previous studies have reported that elevated NF-κB levels enhance Wnt signaling, with de-differentiation of intestinal epithelial cells and the promotion of tumor initiation.[45]

Continued exposure to chronic inflammation can set the stage for development of fibrosis, even cancer. The extracellular matrix (ECM) performs an imperative role during the course of disease. The TLR4 is often aberrantly activated in CAC, which leads to a sustained expansion of the inflammatory response and promotes the progression of CAC. TLR4 further activates the β-catenin pathway, which is involved in ECM formation and plays a central role in proliferation and tumor transformation.[46,47] Studies have shown that inflammation and ECM remodeling can

accelerate the progression of colitis to CAC by affecting hypoxia inducible factor −1α (HIF-1α).[48] HIF-1α expression levels were correlated positively with the expression of β-catenin in cell lines and primary tissues.[49] Some studies have previously reported high activation of stromal HIF-1α expression in CAC, as its promotion in cancer cells was demonstrated to stimulate the release of mTOR and increase glutaminolysis, thus activating tumor metabolism and growth.[50] HIF-1α is activated during the early stages of inflammation in the colon and drives the development of cancer through remodeling of the ECM and fibrosis.[51] Therefore, the TLR4/β-catenin/HIF-1α signaling pathway in AOM/DSS combined-induced CAC may be the key mechanism to induce intestinal fibrosis and CAC progression.

Overall, we build on network pharmacology analysis to construct the animal models of AC, CC and CAC that contribute to preliminarily explore the efficacy and verify the mechanism of QCWZD in the treatment of colitis carcinogenesis. QCWZD could protect the intestinal mucosal barrier, regulate inflammation and improve the process of intestinal fibrosis, that is, QCWZD treatment could ameliorate the development of colitis carcinogenesis from the key pathological mechanism. Results revealed that IL-17A, NF-κB and TLR4/β-catenin/HIF-1α signaling pathways may play a vital role in the therapeutic effect of QCWZD. In terms of limitation of models selection, we have chosen the CAC model, which is established by the combination of AOM and DSS. The entire tumor formation process can be built based on the inflammation. We could consider testing whether QCWZD treatment attenuates inflammation independent sporadic colon cancer models such as C57BL6/J mice carrying the Apc^{Min} mutation. This will also provide more insights into the efficacy of QCWZD on sporadic colon cancer which is the major form of human colorectal cancer. In addition, synergistic effects of components are still unclear. We could screen the superior monomers that enter the blood one by one to prove its function and continue to narrow down the precise protective mechanisms driven by QCWZD in the future studies.

Conclusions

In conclusion, the present study demonstrated that QCWZD can exert its effects on protecting the intestinal mucosal barrier, regulating inflammation and improving intestinal fibrosis by the approach of network pharmacology as well as biological experimental verification. The most prominent mechanism may be related to the activation of the IL-17, NF-κB, and TLR4/β-catenin/HIF-1α signaling pathways.

Data Sharing Statement

The data used to support the findings of this study are available from the corresponding author upon request.

Acknowledgments

This work is supported by the National Key R&D Program of China, Key Research Project of Beijing University of Chinese Medicine. We deeply appreciate all the members of our team.

Author Contributions

All authors made a significant contribution to the work reported, whether that is in the conception, study design, execution, acquisition of data, analysis and interpretation, or in all these areas; took part in drafting, revising or critically reviewing the article; gave final approval of the version to be published; have agreed on the journal to which the article has been submitted; and agree to be accountable for all aspects of the work.

Funding

This work was supported by National Natural Science Foundation of China (82004113); the National Key R&D Program of China [2018YFC1705405], "Jiebang Guashuai" Project of Beijing University of Chinese Medicine (2022-JYB-JBZR-008) and Key Research Project of Beijing University of Chinese Medicine (2020-JYB-ZDGG-125).

Disclosure

The authors report no conflicts of interest in this work.

References

1. Rubin DT, Ananthakrishnan AN, Siegel CA, Sauer BG, Long MD. ACG clinical guideline: ulcerative colitis in adults. *Am J Gastroenterol*. 2019;114(3):384–413. doi:10.14309/ajg.0000000000000152
2. Kobayashi T, Siegmund B, Le Berre C, et al. Ulcerative colitis. *Nat Rev Dis Primers*. 2020;6(1):74. doi:10.1038/s41572-020-0205-x
3. Li X, Gao Y, Yang M, et al. Identification of gene expression changes from colitis to CRC in the mouse CAC model. *PLoS One*. 2014;9(4):e95347. doi:10.1371/journal.pone.0095347
4. Sun Z, Li J, Wang W, et al. Qingchang Wenzhong decoction accelerates intestinal mucosal healing through modulation of dysregulated gut microbiome, intestinal barrier and immune responses in mice. *Front Pharmacol*. 2021;12:738152. doi:10.3389/fphar.2021.738152
5. Shi L, Dai Y, Jia B, et al. The inhibitory effects of Qingchang Wenzhong granule on the interactive network of inflammation, oxidative stress, and apoptosis in rats with dextran sulfate sodium-induced colitis. *J Cell Biochem*. 2019;120(6):9979–9991. doi:10.1002/jcb.28280
6. Ru J, Li P, Wang J, et al. TCMSP: a database of systems pharmacology for drug discovery from herbal medicines. *J Cheminform*. 2014;6:13. doi:10.1186/1758-2946-6-13
7. Daina A, Michielin O, Zoete V. SwissTargetPrediction: updated data and new features for efficient prediction of protein targets of small molecules. *Nucleic Acids Res*. 2019;47(W1):W357–W364. doi:10.1093/nar/gkz382
8. Keiser MJ, Roth BL, Armbruster BN, Ernsberger P, Irwin JJ, Shoichet BK. Relating protein pharmacology by ligand chemistry. *Nat Biotechnol*. 2007;25(2):197–206. doi:10.1038/nbt1284
9. Planell N, Lozano JJ, Mora-Buch R, et al. Transcriptional analysis of the intestinal mucosa of patients with ulcerative colitis in remission reveals lasting epithelial cell alterations. *Gut*. 2013;62(7):967–976. doi:10.1136/gutjnl-2012-303333
10. Bjerrum JT, Nielsen OH, Riis LB, et al. Transcriptional analysis of left-sided colitis, pancolitis, and ulcerative colitis-associated dysplasia. *Inflamm Bowel Dis*. 2014;20(12):2340–2352. doi:10.1097/MIB.0000000000000235
11. Irizarry RA, Hobbs B, Collin F, Beazer-Barclay YD, Antonellis KJ, Scherf U. Exploration, normalization, and summaries of high density oligonucleotide array probe level data. *Biostatistics*. 2003;4(2):249–264. doi:10.1093/biostatistics/4.2.249
12. Ali HR, Chlon L, Pharoah PD, Markowetz F, Caldas C. Patterns of immune infiltration in breast cancer and their clinical implications: a gene-expression-based retrospective study. *PLoS Med*. 2016;13(12):e1002194. doi:10.1371/journal.pmed.1002194
13. Leek JT. svaseq: removing batch effects and other unwanted noise from sequencing data. *Nucleic Acids Res*. 2014;42(21):e161. doi:10.1093/nar/gku864
14. Szklarczyk D, Gable AL, Lyon D, et al. STRING v11: protein-protein association networks with increased coverage, supporting functional discovery in genome-wide experimental datasets. *Nucleic Acids Res*. 2019;47:D607–D613. doi:10.1093/nar/gky1131
15. Zhou Y, Zhou B, Pache L, et al. Metascape provides a biologist-oriented resource for the analysis of systems-level datasets. *Nat Commun*. 2019;10(1):1523. doi:10.1038/s41467-019-09234-6
16. Wirtz S, Popp V, Kindermann M, et al. Chemically induced mouse models of acute and chronic intestinal inflammation. *Nat Protoc*. 2017;12(7):1295–1309. doi:10.1038/nprot.2017.044
17. Sasaki S, Hirata I, Maemura K, et al. Prostaglandin E2 inhibits lesion formation in dextran sodium sulphate-induced colitis in rats and reduces the levels of mucosal inflammatory cytokines. *Scand J Immunol*. 2000;51(1):23–28. doi:10.1046/j.1365-3083.2000.00623.x
18. Cooper HS, Murthy SN, Shah RS, Sedergran DJ. Clinicopathologic study of dextran sulfate sodium experimental murine colitis. *Lab Invest*. 1993;69(2):238–249.
19. Kimura Y, Sumiyoshi M, Kiyoi T, Baba K. Dihydroxystilbenes prevent azoxymethane/dextran sulfate sodium-induced colon cancer by inhibiting colon cytokines, a chemokine, and programmed cell death-1 in C57BL/6J mice. *Eur J Pharmacol*. 2020;886:173445. doi:10.1016/j.ejphar.2020.173445
20. Duan L, Cheng S, Li L, Liu Y, Wang D, Liu G. Natural anti-inflammatory compounds as drug candidates for inflammatory bowel disease. *Front Pharmacol*. 2021;12:684486.
21. Sun Z, Li J, Dai Y, et al. Indigo naturalis alleviates dextran sulfate sodium-induced colitis in rats via altering gut microbiota. *Front Microbiol*. 2020;11:731. doi:10.3389/fmicb.2020.00731
22. Rauf A, Abu-Izneid T, Khalil AA, et al. Berberine as a potential anticancer agent: a comprehensive review. *Molecules*. 2021;26(23):7368. doi:10.3390/molecules26237368
23. Hashemzaei M, Delarami Far A, Yari A, et al. Anticancer and apoptosis inducing effects of quercetin in vitro and in vivo. *Oncol Rep*. 2017;38(2):819–828. doi:10.3892/or.2017.5766
24. Wu H, Cui M, Li C, et al. Kaempferol reverses aerobic glycolysis via miR-339-5p-mediated PKM alternative splicing in colon cancer cells. *J Agric Food Chem*. 2021;69(10):3060–3068. doi:10.1021/acs.jafc.0c07640
25. Lin X, Wang G, Liu P, et al. Gallic acid suppresses colon cancer proliferation by inhibiting SRC and EGFR phosphorylation. *Exp Ther Med*. 2021;21(6):638. doi:10.3892/etm.2021.10070
26. Hirano T, Hirayama D, Wagatsuma K, Yamakawa T, Yokoyama Y, Nakase H. Immunological mechanisms in inflammation-associated colon carcinogenesis. *Int J Mol Sci*. 2020;21(9):3062. doi:10.3390/ijms21093062
27. Moschen AR, Tilg H, Raine T. IL-12, IL-23 and IL-17 in IBD: immunobiology and therapeutic targeting. *Nat Rev Gastroenterol Hepatol*. 2019;16(3):185–196. doi:10.1038/s41575-018-0084-8
28. Hyun YS, Han DS, Lee AR, Eun CS, Youn J, Kim HY. Role of IL-17A in the development of colitis-associated cancer. *Carcinogenesis*. 2012;33:931–936. doi:10.1093/carcin/bgs106
29. Nemati K, Golmoghaddam H, Hosseini SV, Ghaderi A, Doroudchi M. Interleukin-17FT7488 allele is associated with a decreased risk of colorectal cancer and tumor progression. *Gene*. 2015;561(1):88–94. doi:10.1016/j.gene.2015.02.014
30. Grivennikov SI, Wang K, Mucida D, et al. Adenoma-linked barrier defects and microbial products drive IL-23/IL-17-mediated tumour growth. *Nature*. 2012;491(7423):254–258. doi:10.1038/nature11465
31. Xie Z, Qu Y, Leng Y, et al. Human colon carcinogenesis is associated with increased interleukin-17-driven inflammatory responses. *Drug Des Devel Ther*. 2015;9:1679–1689. doi:10.2147/DDDT.S79431
32. Wang S, Liu Z, Wang L, Zhang X. NF-kappaB signaling pathway, inflammation and colorectal cancer. *Cell Mol Immunol*. 2009;6(5):327–334. doi:10.1038/cmi.2009.43

33. Chin CC, Chen CN, Kuo HC, et al. Interleukin-17 induces CC chemokine receptor 6 expression and cell migration in colorectal cancer cells. *J Cell Physiol*. 2015;230(7):1430–1437. doi:10.1002/jcp.24796
34. Numasaki M, Fukushi J, Ono M, et al. Interleukin-17 promotes angiogenesis and tumor growth. *Blood*. 2003;101(7):2620–2627. doi:10.1182/blood-2002-05-1461
35. Chung AS, Wu X, Zhuang G, et al. An interleukin-17-mediated paracrine network promotes tumor resistance to anti-angiogenic therapy. *Nat Med*. 2013;19(9):1114–1123. doi:10.1038/nm.3291
36. Niess JH, Hruz P, Kaymak T. The interleukin-20 cytokines in intestinal diseases. *Front Immunol*. 2018;9:1373. doi:10.3389/fimmu.2018.01373
37. Huber S, Gagliani N, Zenewicz LA, et al. IL-22BP is regulated by the inflammasome and modulates tumorigenesis in the intestine. *Nature*. 2012;491:259–263. doi:10.1038/nature11535
38. Yao D, Dong M, Dai C, Wu S. Inflammation and inflammatory cytokine contribute to the initiation and development of ulcerative colitis and its associated cancer. *Inflamm Bowel Dis*. 2019;25(10):1595–1602. doi:10.1093/ibd/izz149
39. Akira S. Innate immunity and adjuvants. *Philos Trans R Soc Lond B Biol Sci*. 2011;366(1579):2748–2755. doi:10.1098/rstb.2011.0106
40. Kamba A, Lee IA, Mizoguchi E. Potential association between TLR4 and chitinase 3-like 1 (CHI3L1/YKL-40) signaling on colonic epithelial cells in inflammatory bowel disease and colitis-associated cancer. *Curr Mol Med*. 2013;13(7):1110–1121. doi:10.2174/1566524011313070006
41. Lv Z, Wang Z, Luo L, et al. Spliceosome protein Eftud2 promotes colitis-associated tumorigenesis by modulating inflammatory response of macrophage. *Mucosal Immunol*. 2019;12(5):1164–1173. doi:10.1038/s41385-019-0184-y
42. Fukata M, Shang L, Santaolalla R, et al. Constitutive activation of epithelial TLR4 augments inflammatory responses to mucosal injury and drives colitis-associated tumorigenesis. *Inflamm Bowel Dis*. 2011;17(7):1464–1473. doi:10.1002/ibd.21527
43. Fukata M, Chen A, Vamadevan AS, et al. Toll-like receptor-4 promotes the development of colitis-associated colorectal tumors. *Gastroenterology*. 2007;133(6):1869–1881. doi:10.1053/j.gastro.2007.09.008
44. Tenbaum SP, Ordóñez-Morán P, Puig I, et al. β-catenin confers resistance to PI3K and AKT inhibitors and subverts FOXO3a to promote metastasis in colon cancer. *Nat Med*. 2012;18(6):892–901. doi:10.1038/nm.2772
45. Tang F, Cao F, Lu C, He X, Weng L, Sun L. Dvl2 facilitates the coordination of NF-κB and Wnt signaling to promote colitis-associated colorectal progression. *Cancer Sci*. 2021;113:565–575. doi:10.1111/cas.15206
46. Santaolalla R, Sussman DA, Ruiz JR, et al. TLR4 activates the β-catenin pathway to cause intestinal neoplasia. *PLoS One*. 2013;8(5):e63298. doi:10.1371/journal.pone.0063298
47. Stanczak A, Stec R, Bodnar L, et al. Prognostic significance of Wnt-1, β-catenin and E-cadherin expression in advanced colorectal carcinoma. *Pathol Oncol Res*. 2011;17(4):955–963. doi:10.1007/s12253-011-9409-4
48. Han J, Xi Q, Meng Q, et al. Interleukin-6 promotes tumor progression in colitis-associated colorectal cancer through HIF-1α regulation. *Oncol Lett*. 2016;12(6):4665–4670. doi:10.3892/ol.2016.5227
49. Dong S, Liang S, Cheng Z, et al. ROS/PI3K/Akt and Wnt/β-catenin signalings activate HIF-1α-induced metabolic reprogramming to impart 5-fluorouracil resistance in colorectal cancer. *J Exp Clin Cancer Res*. 2022;41(1):15. doi:10.1186/s13046-021-02229-6
50. Chen M, Zhong K, Tan J, et al. Baicalein is a novel TLR4-targeting therapeutics agent that inhibits TLR4/HIF-1α/VEGF signaling pathway in colorectal cancer. *Clin Transl Med*. 2021;11(11):e564. doi:10.1002/ctm2.564
51. Rohwer N, Jumpertz S, Erdem M, et al. Non-canonical HIF-1 stabilization contributes to intestinal tumorigenesis. *Oncogene*. 2019;38(28):5670–5685. doi:10.1038/s41388-019-0816-4